

On the origin of mid-latitude mesospheric clouds: The July 2009 cloud outbreak

Kim Nielsen ^{a,*}, Gerald E. Nedoluha ^b, Amal Chandran ^c, Loren C. Chang ^d, Jodie Barker-Tvedtnes ^e, Michael J. Taylor ^e, Nick J. Mitchell ^f, Alyn Lambert ^g, Michael J. Schwartz ^g, James M. Russell III ^h

^a Computational Physics Inc., Boulder, CO, USA

^b Remote Sensing Division, Naval Research Laboratory, DC, USA

^c Laboratory for Atmospheric and Space Physics, University of Colorado, Boulder, CO, USA

^d Department of Aerospace Engineering Sciences, University of Colorado, Boulder, CO, USA

^e Center for Atmospheric and Space Sciences, Utah State University, UT, USA

^f Centre for Space, Atmospheric and Oceanic Science, University of Bath, UK

^g Jet Propulsion Laboratory, California Institute of Technology, Pasadena, CA, USA

^h Center for Atmospheric Sciences, Hampton University, Hampton, VA, USA

ARTICLE INFO

Article history:

Received 16 February 2010

Received in revised form

3 October 2010

Accepted 24 October 2010

Available online 5 November 2010

Keywords:

Mesospheric clouds

Planetary waves

Mesosphere

ABSTRACT

Mid-latitude mesospheric clouds (MCs) are a rare phenomenon and their existence is not well understood, as the mesosphere at these latitudes is, in general, too warm for clouds to form. During the 2009 northern hemisphere summer season an unusually high number of these clouds were reported over both central and southern Europe, and the western contiguous United States. In this paper we investigate the mesospheric temperature field utilizing data from the Microwave Limb Sounder (MLS) instrument. We find that the temperature occasionally is near the frost point temperature and that the presence of planetary waves with periods of 2-, 5-, and 16-days combine to provide temperature anomalies of 1–1.5 K, lowering the temperature below the frost point for cloud formation and growth. Observed MCs are found to occur in close proximity to the 5-day wave anomaly. Model results show that the growth time to achieve visible particle sizes under the observed temperature and water vapor mixing ratio conditions are greater than ~20 h. Combined with climatological winds from a mid-latitude site, our study suggests that these clouds occur due to a combination of advection from higher and colder latitudes, and in situ wave growth.

© 2010 Elsevier Ltd. All rights reserved.

1. Introduction

Polar mesospheric clouds (PMCs) are a common phenomenon in the polar summer atmosphere, where extremely low temperatures (<130 K) provide a favorable environment for nucleation and growth of these clouds (e.g., Gadsden and Schröder, 1989, and references therein). Recent results have shown an increase of both cloud brightness and occurrence frequency (e.g., Klostermeyer, 2002; DeLand et al., 2007; Shettle et al., 2009). Furthermore, ground-based observers have reported an apparent progression towards mid-latitudes (defined here as observation sites with latitudes below 50°N), where the summer mesopause temperatures in general are well above the frost point temperature (e.g., Wickwar et al., 2002; Yuan et al., 2008). The first reported sighting of a mesospheric cloud (MC) at these lower latitudes occurred in 1999 from Logan, UT (42°N) (Taylor et al., 2002; Wickwar et al., 2002). A later investigation by Herron et al. (2007) showed an earlier cloud

detected with the USU lidar system in June 1995. Since then numerous sightings have been reported by amateur observers on popular web sites such as the noctilucent clouds Observer's Home-page <http://www.kersland.plus.com> and <http://spaceweather.com>, and have revealed observations of MCs at latitudes as low as Palmela, Portugal (~39°N) by P. Casquinha on 29–30 June 2007.

In recent years major effort has been put forward to understand the formation and dynamics of PMCs utilizing a suite of ground-based and satellite observations together with advanced microphysical models. With the recent launch of the Aeronomy of Ice in the Mesosphere (AIM) satellite in 2007, an unprecedentedly detailed study of PMCs is underway (Russell et al., 2009). However, the lower latitude MCs have eluded scientists, due to their rare occurrence. Their origin remains a mystery, as the mid-latitude mesosphere is expected to be too warm to sustain formation and growth of MCs. Mid-latitude observations of MCs have also been observed by the Spatial Heterodyne IMager for Mesospheric Radicals (SHIMMER), which has successfully observed these clouds near 50°N (Stevens et al., 2009). Together with the Navy Operational Global Atmospheric Prediction System Advanced Level Physics High Altitude (NOGAPS-ALPHA) model, a Numerical

* Corresponding author. Tel.: +1 303 4423992.

E-mail address: knelsen@cpi.com (K. Nielsen).

Report Documentation Page			Form Approved OMB No. 0704-0188	
<p>Public reporting burden for the collection of information is estimated to average 1 hour per response, including the time for reviewing instructions, searching existing data sources, gathering and maintaining the data needed, and completing and reviewing the collection of information. Send comments regarding this burden estimate or any other aspect of this collection of information, including suggestions for reducing this burden, to Washington Headquarters Services, Directorate for Information Operations and Reports, 1215 Jefferson Davis Highway, Suite 1204, Arlington VA 22202-4302. Respondents should be aware that notwithstanding any other provision of law, no person shall be subject to a penalty for failing to comply with a collection of information if it does not display a currently valid OMB control number.</p>				
1. REPORT DATE OCT 2010	2. REPORT TYPE	3. DATES COVERED 00-00-2010 to 00-00-2010		
4. TITLE AND SUBTITLE On the origin of mid-latitude mesospheric clouds: The July 2009 cloud outbreak			5a. CONTRACT NUMBER	5b. GRANT NUMBER
			5c. PROGRAM ELEMENT NUMBER	5d. PROJECT NUMBER
			5e. TASK NUMBER	5f. WORK UNIT NUMBER
7. PERFORMING ORGANIZATION NAME(S) AND ADDRESS(ES) Naval Research Laboratory, Remote Sensing Division, Washington, DC, 20375			8. PERFORMING ORGANIZATION REPORT NUMBER	
9. SPONSORING/MONITORING AGENCY NAME(S) AND ADDRESS(ES)			10. SPONSOR/MONITOR'S ACRONYM(S)	
			11. SPONSOR/MONITOR'S REPORT NUMBER(S)	
12. DISTRIBUTION/AVAILABILITY STATEMENT Approved for public release; distribution unlimited				
13. SUPPLEMENTARY NOTES				
<p>14. ABSTRACT</p> <p>Mid-latitude mesospheric clouds (MCs) are a rare phenomenon and their existence is not well understood, as the mesosphere at these latitudes is, in general, too warm for clouds to form. During the 2009 northern hemisphere summer season an unusually high number of these clouds were reported over both central and southern Europe, and the western contiguous United States. In this paper we investigate the mesospheric temperature field utilizing data from the Microwave Limb Sounder (MLS) instrument. We find that the temperature occasionally is near the frost point temperature and that the presence of planetary waves with periods of 2-, 5-, and 16-days combine to provide temperature anomalies of 1?1.5K, lowering the temperature below the frost point for cloud formation and growth. Observed MCs are found to occur in close proximity to the 5-day wave anomaly. Model results show that the growth time to achieve visible particle sizes under the observed temperature and water vapor mixing ratio conditions are greater than 20 h. Combined with climatological winds from mid-latitude sites our study suggests that these clouds occur due to a combination of advection from higher and colder latitudes, and in situ wave growth.</p>				
15. SUBJECT TERMS				
16. SECURITY CLASSIFICATION OF:			17. LIMITATION OF ABSTRACT Same as Report (SAR)	18. NUMBER OF PAGES 7
a. REPORT unclassified	b. ABSTRACT unclassified	c. THIS PAGE unclassified	19a. NAME OF RESPONSIBLE PERSON	

Weather Prediction (NWP) system extending into mesosphere and lower thermosphere, SHIMMER has shown promise in resolving the mystery behind MC formation (Eckermann et al., 2009).

During the 2009 northern hemispheric summer, a large outburst of MCs was observed over a large part of Europe and the contiguous western United States, spanning the time period from 13 to 15 July. Intriguingly, ~5–6 days later MCs were again observed over Europe. It is well known that planetary waves, and in particular the 5-day wave, can largely impact PMC formation and dynamics in the polar atmosphere (e.g., Kirkwood et al., 2002; Kirkwood and Stebel, 2003; Merkel et al., 2003, 2008, 2009; Nielsen et al., 2010; von Savigny et al., 2007). In fact, Nielsen et al. (2010) showed that during the late polar mesospheric summer, when the zonal mean temperature is well above the frost point, the 5-day wave can induce cold periods with cloud formation lasting 2–3 days corresponding to the cold phase of the wave. These late season temperature conditions are similar to those observed at mid-latitudes. In this paper, we investigate the presence of planetary waves at mid-latitudes, during the MC observations, and whether the associated perturbations can explain the observed clouds. We show that the observed clouds during the 2009 season, to a large degree, can be understood in terms of planetary wave effects and that enhanced 5-day wave activity occurred during the July outbursts of MCs.

2. Observations

The 2009 northern hemisphere summer provided an unprecedented number of reported mid-latitude ($< 50^{\circ}$ N) MC observations. According to the reports at <http://www.kersland.plus.com> and <http://spaceweather.com> a total number of 68 cloud observations were made with the lowest observation site being Coal Creek Canyon, Colorado ($\sim 40^{\circ}$ N) on 15 July. All of the reported observations occurred over Europe or the western United States (US). Eighteen observations were reported during the month of June, only one of which (from Logan, UT (42° N) on June 23) was from a US site. In contrast, July yielded 50 cloud observations with 25 over the US and a majority of the July observations occurring in the time period of 13–15 July (38 observations out of 50). The 2007 northern summer had the next highest number of reported observations with 18 (lowest latitude $\sim 39^{\circ}$ N). However, these reports must be evaluated scientifically with care as they are dependent on many factors, such as numbers of observers, visibility, and the fact that observations made in close proximity of each other likely observe the same cloud system. Here, we are merely using the reports as a proxy to show the extent of mid-latitude clouds. Fig. 1 shows an example of mid-latitude MC displays captured from Logan, UT (top) and Rawlins, WY ($\sim 42^{\circ}$ N) (bottom) on July 15, 2009. The cloud fields are broad in E–W direction and extend ~ 8 – 10° in elevation, putting the closest clouds at $\sim 48^{\circ}$ N.

Climatological descriptions of the mid-latitude mesosphere generally have temperatures too high for the formation and growth of MCs (e.g., Yuan et al., 2008). To investigate the mid-latitude mesospheric capability to form MCs during the 2009 summer, we utilize temperature and water vapor measurements from the MLS instrument on board the Aura satellite to determine whether the air reached super-saturated levels. The satellite was launched in 2004 into a near-polar 705 km altitude sun-synchronous orbit providing daily global coverage with ~ 14 orbits per day yielding a longitudinal resolution of $\sim 12^{\circ}$ at mid-latitudes (Schwartz and et al., 2008). The latest publicly released MLS data product (v2.2) has a temperature vertical resolution of 14 km, along track resolution of ~ 200 km, and 12 km cross-track at 0.0046 hPa (Schwartz and et al., 2008), which is the approximate level (~ 84 km) of observed mid-latitude MCs. The temperature has a known warm bias of ~ 2 K, which has been subtracted in our analysis. The vertical

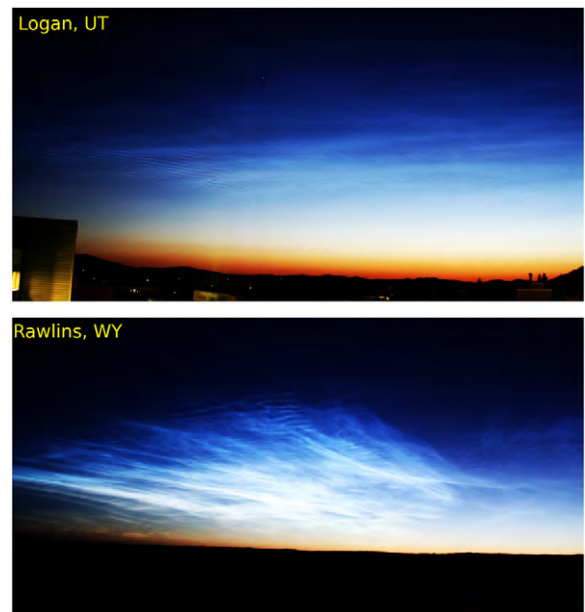


Fig. 1. This figure shows two extensive displays captured from Logan, UT (top) and near Rawlins, WY (bottom) (both at $\sim 42^{\circ}$ N) on the night of 14/15 July, 2009. The NLC displays extended across the camera's horizontal fields of view ($\sim 63^{\circ}$) and ~ 8 – 10° in elevation.

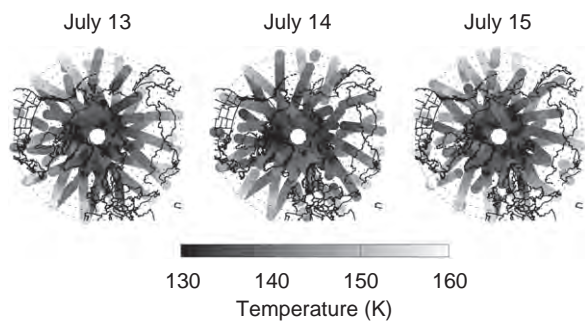


Fig. 2. The MLS temperature observations shown on 13, 14, and 15 July, 2009. The altitude is 0.0046 hPa corresponding to ~ 84 km.

resolution for water vapor is ~ 15 km, 400–750 km along track and 7 km cross-track (Lambert and et al., 2007).

Fig. 2 shows MLS temperature observations for 13–15 July, the period of the cloud outburst. The figure shows the expected cold polar summer mesosphere with temperatures down to 130 K. However, the plots also reveal a cold mid-latitude region with temperatures below 150 K ranging from $\sim 20^{\circ}$ E to 110° W on 13 July. Similar characteristics are observed on 14 July, whereas on 15 July the cold pattern appears to have progressed westward to cover the 110° E to 150° E region.

3. Analysis and discussion

To exploit the mid-latitude MLS temperature and water vapor fields, and their variations over the course of the main summer season, Fig. 3 shows the daily averaged fields (including both ascending and descending node data) over the 48° – 55° N latitude band in Hovmöller form (time versus longitude) in 10° longitude bins. The latitudinal band was chosen to be consistent with the spatial extend of the clouds shown in Fig. 1, and to coincide with the latitude band of the majority of the ground-based observations. The temperature is shown in (a), the water vapor in (b), and derived

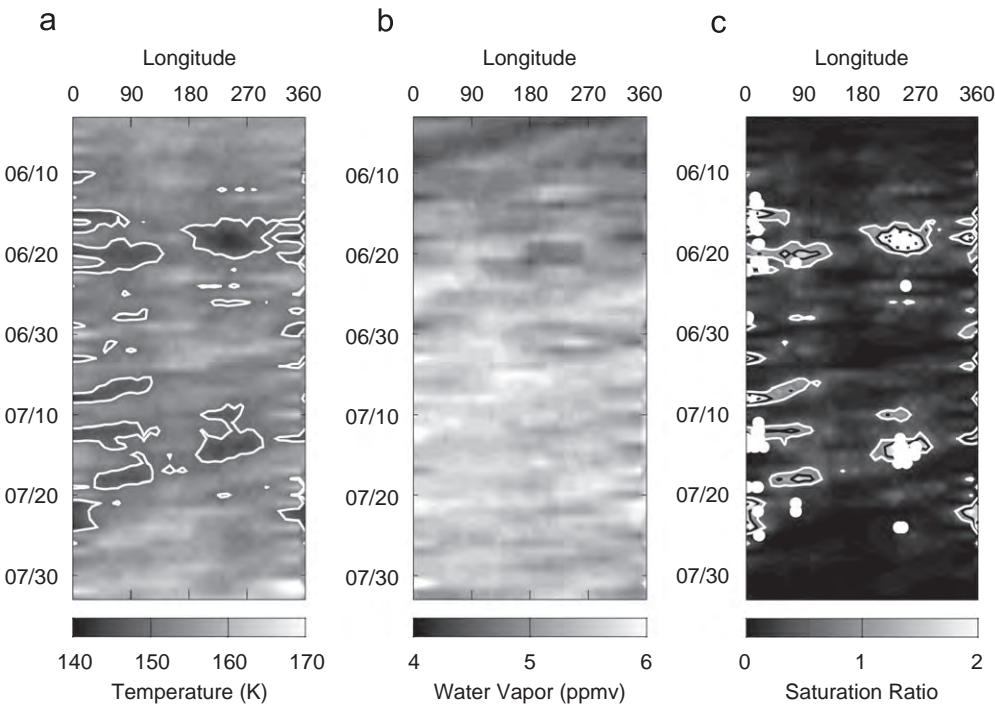


Fig. 3. Hovmöller plot of daily averaged MLS temperature (a) averaged across the 48°–55° latitude band at the 0.0046 hPa level with the white contour lines representing the 150 K level. In (b) is shown the water vapor, while (c) shows the derived saturation ratio with super-saturated air enclosed by the black contour lines. Super-saturated air for ± 2 K perturbations are also shown (white and black dot contours) to illustrate the sensitivity to temperature variations at these latitudes during the summer period. The reported MC observations are shown as white circles.

saturation ratio is shown in (c). The saturation ratio is defined as the ratio between the partial pressure of water vapor and the partial pressure over ice:

$$S = \frac{p_{H_2O}}{p_{ice}}. \quad (1)$$

The partial pressure of water vapor is simply

$$p_{H_2O} = p \cdot \chi_{H_2O}, \quad (2)$$

where p is the ambient pressure and χ is the water vapor mixing ratio in ppmv. Here, we follow the recommendations of Rapp and Thomas (2006) by using the formula determined by Murphy and Koop (2005) to derive the partial pressure of ice, as it is valid for temperatures above 110 K and thus valid for mesospheric cloud studies.

Fig. 3a shows two relatively extensive periods exhibiting temperatures near the frost point, between ~ 15 – 20 June, where the majority of the June observations occurred and ~ 10 – 20 July encompassing the July cloud outbreak. The two periods are borderline for cloud formations exhibiting similar temperature conditions, as the late summer (early August) polar mesosphere (e.g., Nielsen et al., 2010). Nielsen et al. (2010) showed that PMCs observed during the late polar summer were a result of temperature perturbations due to the 5-day wave inducing favorable PMC conditions, although the zonal mean temperature was significantly above the frost point. Interestingly, Fig. 3a shows sporadic striations resembling a westward propagating wave 1 with period of ~ 5 -days. Fig. 3b shows water vapor mixing ratios, which peak in summer at high latitudes in the mesosphere (e.g., Eckermann et al., 2009; Nielsen et al., 2010), where these clouds occur frequently during the mid summer period. The saturation ratio shown in Fig. 3c has been shown to be a good proxy for PMC existence (Eckermann et al., 2009; Nielsen et al., 2010), and here shows localized regions of super-saturated air ($S > 1$) as indicated by the black contour lines. However, as the temperature field is close to

the frost point temperature, the conditions for super-saturation are very sensitive to temperature variations. This is illustrated by the white and black dot contours showing the saturation for a ± 2 K perturbation. A majority of the saturation field is well below the required level for MC formation and illustrates the rarity and sporadic occurrence of the clouds at these latitudes.

The localized regions of super-saturated air intriguingly appear preferably within two longitude regions ($\sim 340^\circ$ – 100° E and $\sim 180^\circ$ – 270° E). It is noteworthy to mention that Herron et al. (2007) stated that only the lidar operating at Utah State detected the cloud in 1995, whereas the other mid-latitude lidar systems measured none. That lead Herron et al. (2007) to speculate on longitudinal effects, such as orographic waves from the Rocky Mountains, non-migrating tides, or stationary planetary waves over the mountainous region. Our observations suggest a similar longitudinal preference, although not limited to the western USA but also including the European sector, pointing towards large-scale mechanisms for the longitudinal preference.

There are indications of the super-saturated regions in July occurring along the striations observed in the temperature field, pointing towards planetary wave activity as a driver behind these MC favorable regions. The reported MC observations are shown as white circles. It is evident that a majority of the observations (64 out of 68) occurs within, or in close proximity to, super-saturated regions, showing that the derived saturation is a good proxy for MCs.

In the following, we will analyze the saturation field to determine the existence of planetary waves and how they may impact the observed clouds, utilizing a wavelet analysis technique developed by Torrence and Compo (1998). This analysis has previously been used to study planetary wave activity and evolution of the 5-day wave in PMCs (von Savigny et al., 2007; Nielsen et al., 2010).

To perform a wavelet analysis, daily averaged MLS data has been binned in 10° longitude and averaged across the 48° – 55° . By performing a 1-D wavelet transform to the saturation time series shown in Fig. 3c at each longitude point, Fig. 4 shows the

normalized saturation wavelet power averaged over all longitudes for periods ranging from 2 to 30 days. The wavelet power is normalized by the variance of the time series and the 95% confidence levels are bounded by the black contour lines. The background spectrum to a good approximation resembles white noise and the confidence levels are determined using the methodology described by [Torrence and Compo \(1998\)](#) with a lag-1 autocorrelation value of 0. The strongest signals occur with a period ~ 5 -days and correspond to the gravest planetary wave normal mode (e.g., [Forbes, 1995](#)). Peaks are also observed at ~ 2 - and 15-days corresponding to the quasi 2- and 16-day waves. The 2-day wave exhibits three localized peaks, with the two first peaks in close proximity in time with the 5-day peaks covering the periods 10–20 June and 30 June–15 July. The 16-day signal is less localized in scale with its major peak occurring during 10–25 July, with a wide spectral response from ~ 12 –24 days. It is possible that the 16-day signal is being masked by a longer period signal, such as the 27-day solar signature, which most recently has been reported in PMCs by [Robert et al. \(2010\)](#). Based on the major peaks identified in this figure, we define the bandwidths for the quasi 2-, 5-, and the 16-day waves as 2.0–2.9, 4.1–7.6, and 12.0–21.5 days, respectively.

[Fig. 5](#) shows the bandpass filtered 2- (a), 5- (b), and 16-day (c) saturation ratio wave amplitudes in Hovmöller form. The reported

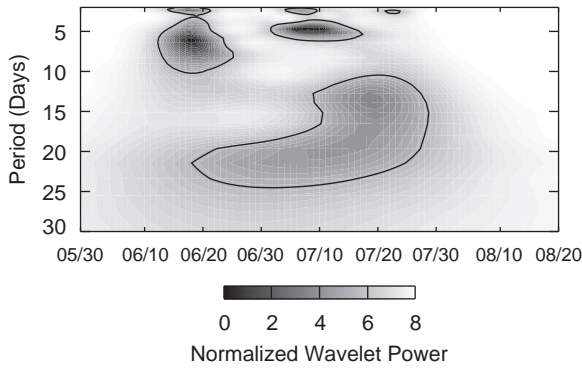


Fig. 4. This plot shows the normalized saturation wavelet power spectrum calculated for each longitude shown in [Fig. 3](#) and then averaged over all longitudes. The 95% confidence levels are indicated by black contours.

cloud observations are shown as open circles. It is clear from (a), (b), and (c), that the wavelet power peaks in [Fig. 4](#) are not only localized in time, but also in space, as the strongest wave amplitudes occur in narrow longitude bands around 0° E and 270° E. The regions where super-saturated air is seen in [Fig. 3c](#) generally correlate with regions where the 2-, 5-, and 16-day wave have the largest amplitudes. Furthermore, a majority of the reported MC observations falls within the regions of stronger wave amplitudes, strongly suggesting that planetary wave activity played a major role in forming these mid-latitude clouds during the 2009 northern hemispheric summer season. As the wavelet transform retains phase at each longitude, [Fig. 5b](#) shows a clear westward propagating wave 1 signal associated with the wave structures signals during mid July, while the earlier wave structures are less coherent. The 2-day wave exhibits saturation ratio peak amplitudes up to ~ 0.5 , while the 5-day anomaly is more extensive and exhibits a twice as large peak amplitude of ~ 1 . This is a significant amplitude, considering the relatively extensive regions of super-saturation levels $S=1$ shown in [Fig. 3c](#). The 16-day wave amplitude is significantly less with peak values of ~ 0.2 .

The clouds respond to the net saturation, and in [Fig. 6](#) we show the combined effects of the three waves. During the relatively few clouds in June (as compared to July), it is evident that there is no clear relationship between the wave activity and the reported cloud observations, as only $\sim 50\%$ occurs within a positive perturbation. It is surprising to note the lack of cloud observations between ~ 200 – 270° E, as this region exhibits the highest perturbation and most extensive region of super-saturated air (cf. [Fig. 3c](#)). However, this may be a reflection of a lack of NLC observations, either due to no observers or extensive tropospheric cloud cover. Hence, our study illustrates the importance of an extensive and continuous observing network, during the summer months, at these latitudes.

In contrast, the outbreak of MCs over Europe on 12–14 July, to a large degree, falls within a positive perturbation, resembling the more dominant 5-day signature. As the disturbance propagates westward, it intensifies ~ 2 days later over the western US, where the majority of the reported cloud observations occurs in conjunction with the overall positive perturbation. Here, the perturbation is driven mainly by the 5-day wave and, to a smaller extent, the 2- and 16-day waves. On 13 July, all three waves exhibit positive perturbations, whereas on 14 July only the 5- and 16-day waves are enforcing each other, and the 2-day wave exhibits a negative

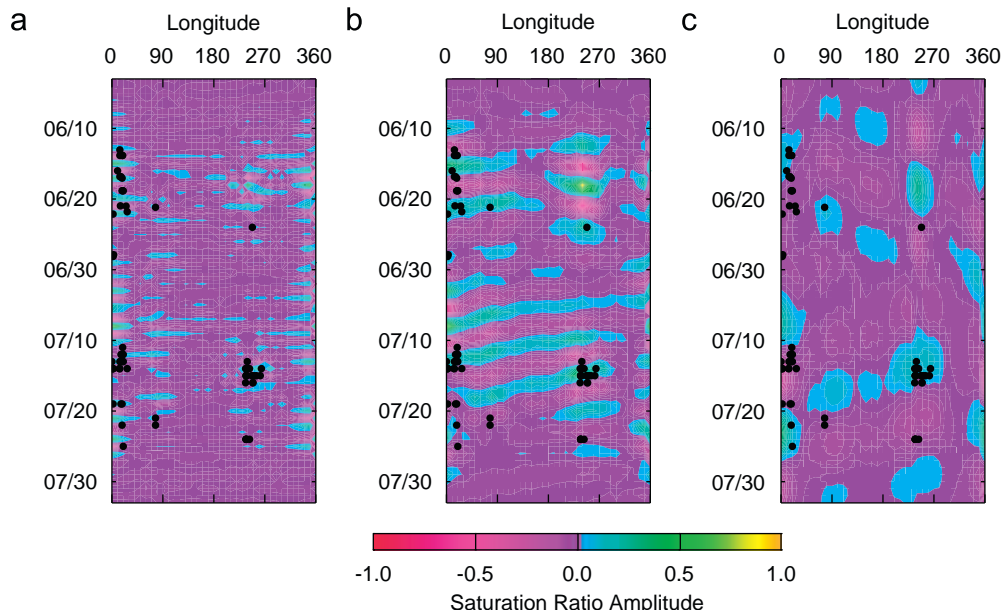


Fig. 5. The 2- (a), 5- (b), 16-day (c) saturation ratio amplitudes shown in Hovmöller form. The 68 reported cloud observations are shown as open black circles.

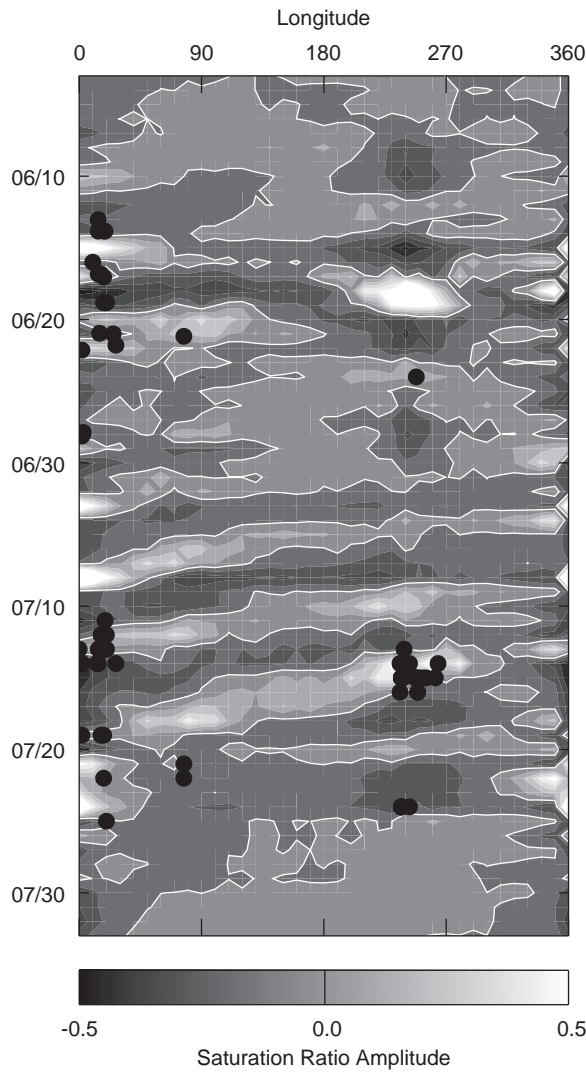


Fig. 6. This figure shows the combined signal of the three planetary wave signals shown in Fig. 5. The white contour lines illustrate the $S=0$ boundaries, while the black circles represent the cloud observations.

perturbation. However, the overall perturbation is positive on both days and is indicative of the fact that the waves are responsible for keeping the air super-saturated for an extended period of time (~ 2 days), possibly providing enough time for MC formation and growth. On 15 July, both the 2- and 5-day waves are exhibiting near zero amplitude (the 16-day wave is still in the positive perturbation phase, but with very weak amplitude) resulting in a near zero overall perturbation, which coincides with the transition from super-saturated into sub-saturated air. On 16 July, observations were still made from Logan, UT without any positive cloud identifications, suggesting the cloud field no longer existed.

The remaining part of the season exhibits a more complex behavior. This complexity cannot be accounted for by planetary wave motion and illustrates that much is still to be learned about these mid-latitude clouds. Other dynamic features to consider are advection of clouds from higher latitudes and large-scale outbreaks of cold mesospheric regions.

Fig. 5 qualitatively suggests the majority of the observed clouds to fall within the positive 5-day saturation anomaly. Fig. 7 illustrates a more quantitative analysis of the dominant 5-day influence in form of a histogram showing the number of reported observations as a function of the 5-day saturation wave phase. The phases associated with positive perturbations are shaded grey. The figure

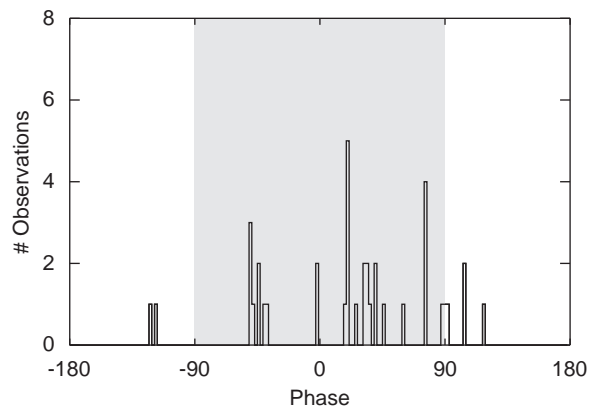


Fig. 7. A histogram showing the number of cloud observations as a function of the 5-day saturation phases. The grey region represents the positive perturbations.

shows that the majority of the observations occur within the enhanced 5-day saturation anomaly ($\sim 75\%$) thus confirming the qualitative results from Fig. 5. Furthermore, it is also evident that more clouds are found in the later stage of the positive phase. A possible explanation for this behavior is that clouds growing in the early stage of the super-saturated phase are sub-visible and first reach visible sizes during the later phase stage, suggesting a relatively slow growth process.

We have shown that planetary wave activity, and in particular the 5-day wave, is responsible for the cold mesospheric temperature fields existing in mid-July, at mid-latitudes, providing an environment of saturated air required for the existence of mesospheric clouds. The origin of these clouds is still not determined. In situ generation in the cold phases of these waves is one possibility. However, the saturated regions are less extensive than the higher latitude counterparts (Nielsen et al., 2010) and may not be temporally extensive to fully grow these clouds. The previous lower mid-latitude MC events discussed in the literature (Wickwar et al., 2002; Taylor et al., 2002; Herron et al., 2007) suggested several origins of these clouds: increased gravity wave activity leading to increased zonal wave-drag and hence mesospheric cooling, or cold temperature perturbations, due to orographic wave forcing from the Rocky Mountains. In particular, Herron et al. (2007) observed a large-amplitude wave (~ 15 K) resembling the diurnal tide in conjunction with the observed cloud.

To investigate the possibility of in situ cloud formation, we have employed the two-dimensional version of the Community Aerosol and Radiation Model for Atmospheres (CARMA). A one-dimensional version of CARMA was first used by Turco et al. (1982), and most recently by Rapp and Thomas (2006) to study the physics of mesospheric ice particles. Jensen and Thomas (1994) and Rapp et al. (2002) have previously used the two-dimensional version of CARMA to investigate mesospheric cloud formation and evolution. The model is initialized with temperature profiles from the Sounding of the Atmosphere using Broadband Emission Radiometry (SABER) instrument onboard the Thermosphere, Ionosphere, Mesosphere Energetics and Dynamics (TIMED) spacecraft and water vapor profiles from MLS measurements for 12–13 July 2009, averaged over a 5° latitude band centered at the 55°N . SABER temperature measurements on 14 July are not included, due to the yaw maneuver occurring on that day.

Fig. 8 shows the temporal evolution of temperature, water vapor, and mean ice particle radius in the MC region (80–90 km), as predicted by CARMA. Fig. 8a shows a mesopause with minimum temperatures of ~ 145 K, around an altitude of 85 km. The water vapor profile in Fig. 8b shows the water being depleted and redistributed in the MC region, as ice formation takes place.

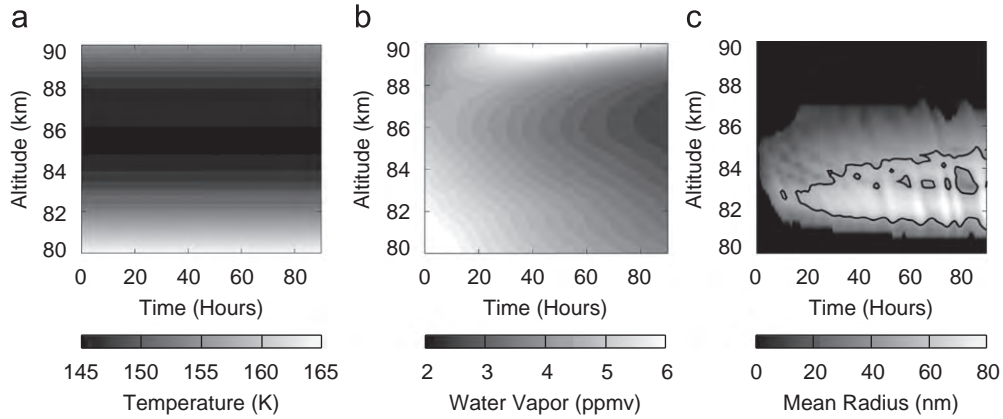


Fig. 8. CARMA model results showing the temperature (a) water vapor (b) mean radius (c) with the black contour showing the 50 nm radius.

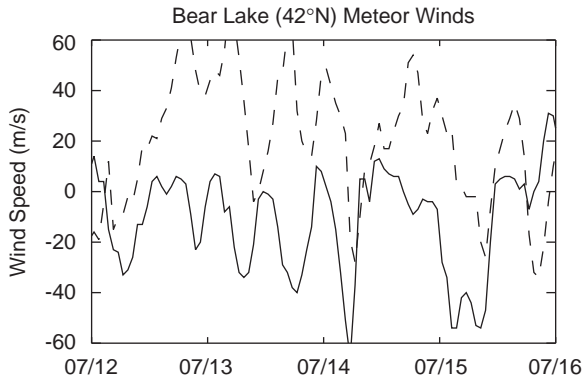


Fig. 9. This figure shows the hourly averaged meteor radar winds measured at ~ 85 km over Bear Lake, UT, from 12 to 16 July 2009. The solid line shows the meridional wind and the zonal wind is shown by the dashed line.

The initial ice particle growth takes place mostly near the mesopause between 85 and 87 km, and the ice particles grow bigger as they sediment down, towards the sublimation level near 81 km. The mean radius plot in Fig. 8c shows ice particles growing as large as up to ~ 80 nm in size after ~ 60 h. MCs visible to the naked eye require relatively large particles. Although there is no consensus in the scientific community on the particle size of a bright cloud, we adopt the value of 50 nm to represent bright clouds, which is similar to the value used by Baumgarten et al. (2009). According to Fig. 8c, this particle population (enclosed by the black contours) appears after ~ 18 h. It is important to keep in mind that these growth times represent a lower limit, as the temperature is kept constant in the model, whereas the wave-induced temperatures change with wave period. With this knowledge, Fig. 8c shows that the quasi 2-day wave (wavenumbers 2 and 3) is not a likely candidate to persistently grow particles with radius ~ 50 nm, and thus may explain the lack of direct correlation between observed clouds and 2 day saturation anomaly in Fig. 5a. In contrast, the quasi 5-day wave (wavenumber 1) has the potential to grow large particles up to ~ 70 nm in situ and may explain the large number of clouds found within the negative saturation anomaly in Fig. 5b. The longer period, 16-day anomaly, seen in Fig. 5c is not likely to play a dominant role in cloud formation, as it exhibits an order of magnitude lower amplitudes.

A comprehensive spatial and temporal wind field is not available to fully investigate the role of advection during the July 2009 cloud outbreak. However, the meteor radar located at Bear Lake Observatory (42°N , 111°W) acquired mesospheric wind data during the period of NLC observations. The hourly averaged zonal (dash) and meridional (solid) winds, at an altitude of 85 km, are shown in Fig. 9. It

is evident that there exists a predominantly equatorward wind field exhibiting peak amplitudes of ~ 40 m/s and mean of ~ 10 m/s, during the cloud outbreak. In comparison, Yuan et al. (2008) reported a 4 year climatology of the meridional wind field above Fort Collins, Colorado (41°N , 105°W), over the period 2002–2006 utilizing a Na lidar. Their results showed a July monthly mean equatorward meridional wind field of ~ 6 m/s. These observations imply that over the course of a cold 5-day temperature perturbation, a cloud could potentially migrate a significant distance equatorward from higher (and presumably, colder) latitudes, assuming the reported wind amplitudes are representative over a larger latitudinal band extending towards higher latitudes.

4. Summary

We have utilized MLS temperature and water vapor to derive the saturation ratio, which acts as a proxy for mesospheric clouds, over a latitude band (48° – 55°N) at 0.0046 hPa during the 2009 summer. The temperature field exhibits periods of unusually low temperatures (< 150 K), which induces regions of super-saturated air. Wavelet analysis of the saturation field reveals sporadic burst of planetary wave activity, exhibiting periods corresponding to the quasi 2-, 5-, and 16-day wave modes.

Our results show that the outbreak of mid-latitude mesospheric clouds in mid-July 2009 was due to additional cooling, as the 2-, 5-, and 16-day planetary waves combined to lower the mesospheric temperature below the frost point. This cooling provided an environment in favor of forming these rare clouds. Locations of reported observations of MCs were compared to these outbreaks of super-saturated air and showed the clouds to dominantly fall within the 5-day high saturation anomaly during the July outbreak, suggesting the 5-day wave was the most dominant driver behind these clouds.

Model results initialized using SABER temperatures and MLS water vapor show that the 2-day wave falls short of growing visible MCs, whereas the 5-day wave has the potential to grow the clouds in situ and thus explains the strong correlation between the observed clouds and the 5-day anomaly. Mid-latitude radar winds reveal a predominantly equatorward wind field capable of transporting the clouds from higher, and colder latitudes, suggesting that advection from higher latitudes may also play a role in the appearance of these mid-latitude clouds.

Acknowledgments

The authors would like to acknowledge all NLC observers who provide invaluable information to the public community through

<http://www.kersland.plus.com> and <http://spaceweather.com>. Wavelet software was partly provided by C. Torrence and G. Compo, and is available at URL: <http://atoc.colorado.edu/research/wavelets/>. Work at the Jet Propulsion Laboratory, California Institute of Technology, was carried out under a contract with the National Aeronautics and Space Administration.

References

Baumgarten, G., Fiedler, J., Fricke, K.H., Gerdling, M., Hervig, M., Hoffmann, P., Müller, N., Pautet, P.-D., Rapp, M., Robert, C., Rusch, D., von Savigny, C., Singer, W., 2009. The noctilucent cloud (NLC) display during the ECOMA/MASS sounding rocket flights on 3 August 2007: morphology on global to local scales. *Ann. Geophys.* 27, 953–965.

DeLand, M.T., Shettle, E.P., Thomas, G.E., Olivero, J.J., 2007. Latitude-dependent long-term variations in polar mesospheric clouds from SBUV version 3 PMC data. *J. Geophys. Res.* 112, D10315. doi:10.1029/2006JD007857.

Eckermann, S.D., Hoppel, K.W., Coy, L., McCormack, J.P., Siskind, D.E., Nielsen, K., Kochenash, A., Stevens, M.H., Englert, C.R., Hervig, M.E., 2009. High-altitude data assimilation system experiments for the northern summer mesosphere season of 2007. *J. Atmos. Sol. Terr. Phys.* 71 (3–4), 531–551. doi:10.1016/j.jastp.2008.09.036.

Forbes, J.M., 1995. Tidal and planetary waves. In: Johnson, R.M., Killeen, T.L. (Eds.), *The Upper Mesosphere and Lower Thermosphere: A Review of Experiment and Theory*, Geophysics Monograph Series, vol. 87. AGU, Washington, DC, pp. 67–87.

Gadsden, M., Schröder, W., 1989. Noctilucent clouds. *Physics and Chemistry in Space*, vol. 18. Springer-Verlag, Berlin.

Herron, J.P., Wickwar, V.B., Espy, P.J., Meriwether, J.W., 2007. Observations of noctilucent cloud above Logan, Utah (41.7°N, 111.8°W) in 1995. *J. Geophys. Res.* 112, D19203. doi:10.1029/2006JD007158.

Jensen, E.J., Thomas, G.E., 1994. Numerical simulations of the effects of gravity waves on noctilucent clouds. *J. Geophys. Res.* 99 (D2), 3421–3430.

Kirkwood, S., Barabash, V., Brändström, B.U.E., Moström, A., Stebel, K., Mitchell, N., Hocking, W., 2002. Noctilucent clouds, PMSE and 5-day planetary waves: a case study. *Geophys. Res. Lett.* 29 (10), 1411. doi:10.1029/2001GL014022.

Kirkwood, S., Stebel, K., 2003. Influence of planetary waves on noctilucent cloud occurrence over NW Europe. *J. Geophys. Res.* 108 (D8), 8440. doi:10.1029/2002JD002356.

Klostermeyer, J., 2002. Noctilucent clouds getting brighter. *J. Geophys. Res.* 107 (D14), 4195. doi:10.1029/2001JD001345.

Lambert, A., et al., 2007. Validation of the Aura Microwave Limb Sounder middle atmosphere water vapor and nitrous oxide measurements. *J. Geophys. Res.* 112, D24S36. doi:10.1029/2007JD008724.

Merkel, A.W., Thomas, G.E., Palo, S.E., Bailey, S.M., 2003. Observations of the 5-day planetary wave in PMC measurements from the Student Nitric Oxide Explorer Satellite. *Geophys. Res. Lett.* 30 (4), 1196. doi:10.1029/2002GL016524.

Merkel, A.W., Garcia, R.R., Bailey, S.M., Russell III, J.M., 2008. Observational studies of planetary waves in PMCs and mesospheric temperature measured by SNOE and SABER. *J. Geophys. Res.* 113, D14202. doi:10.1029/2007JD009396.

Merkel, A.W., Rusch, D.W., Palo, S.E., Russell III, J.M., Bailey, S.M., 2009. Mesospheric planetary wave activity inferred from AIM-CIPS and TIMED-SABER for the northern summer 2007 PMC season. *J. Atmos. Sol. Terr. Phys.* 71 (3–4), 381–391. doi:10.1016/j.jastp.2008.12.001.

Murphy, D.M., Koop, T., 2005. Review of the vapour pressures of ice and supercooled water for atmospheric applications. *Q. J. R. Meteorol. Soc.* 131, 1539–1565.

Nielsen, K., Siskind, D.E., Eckermann, S.D., Hoppel, K.W., Coy, L., McCormack, J.P., Benze, S., Randall, C.E., Hervig, M.E., 2010. Seasonal variation of the quasi 5 day planetary wave: causes and consequences for polar mesospheric cloud variability in 2007. *J. Geophys. Res.* 115, D18111. doi:10.1029/2009JD012676.

Rapp, M., Lübken, F.-J., Müllermann, A., Thomas, G.E., Jensen, E.J., 2002. Small-scale temperature variations in the vicinity of NLC: experimental and model results. *J. Geophys. Res.* 107 (D19), 4392. doi:10.1029/2001JD001241.

Rapp, M., Thomas, G.E., 2006. Modeling the microphysics of mesospheric ice particles: assessment of current capabilities and basic sensitivities. *J. Atmos. Sol. Terr. Phys.* 68, 715–744.

Robert, C.E., von Savigny, C., Rahpoe, N., Bovensmann, H., Burrows, J.P., DeLand, M.T., Schwartz, M.J., 2010. First evidence of a 27 day solar signature in noctilucent cloud occurrence frequency. *J. Geophys. Res.* 115, D00112. doi:10.1029/2009JD012359.

Russell III, J.M., et al., 2009. Aeronomy of ice in the mesosphere (AIM): overview and early science results. *J. Atmos. Sol. Terr. Phys.* 71 (3–4), 289–299. doi:10.1016/j.jastp.2008.08.011.

Schwartz, M.J., et al., 2008. Validation of the Aura Microwave Limb Sounder temperature and geopotential height measurements. *J. Geophys. Res.* 113, D15S11. doi:10.1029/2007JD008783.

Shettle, E.P., DeLand, M.T., Thomas, G.E., Olivero, J.J., 2009. Long term variations in the frequency of polar mesospheric clouds in the Northern Hemisphere from SBUV. *Geophys. Res. Lett.* 36, L02803. doi:10.1029/2008GL036048.

Stevens, M.H., Englert, C.R., Hervig, M., Petelina, S.V., Singer, W., Nielsen, K., 2009. The diurnal variation of polar mesospheric cloud frequency near 55°N observed by SHIMMER. *J. Atmos. Sol. Terr. Phys.* 71 (3–4), 401–407. doi:10.1016/j.jastp.2008.10.009.

Taylor, M.J., Gadsden, M., Lowe, R.P., Zalcik, M.S., Brausch, J., 2002. Mesospheric cloud observations at unusually low latitudes. *J. Atmos. Sci.* 64, 991–999.

Torrence, C., Compo, G.P., 1998. A practical guide to wavelet analysis. *Bull. Am. Meteorol. Soc.* 79, 61–78.

Turco, R.P., Toon, B.O., Whitten, R.C., Keesee, R.G., Hollenback, D., 1982. Noctilucent clouds: simulation studies of their genesis, properties and global influences. *Planet. Space Sci.* 30, 1147–1181.

von Savigny, C., Robert, C., Bovensmann, H., Burrows, J.P., Schwartz, M., 2007. Satellite observations of the quasi 5-day wave in noctilucent clouds and mesopause temperatures. *Geophys. Res. Lett.* 34, L24808. doi:10.1029/2007GL030987.

Wickwar, V.B., Taylor, M.J., Herron, J.P., Martineau, B.A., 2002. Visual and lidar observations of noctilucent clouds above Logan, at 41.7°N. *J. Geophys. Res.* 107 (D7), 4054. doi:10.1029/2001JD001180.

Yuan, T., She, C.-Y., Kruger, D.A., Sassi, F., Garcia, R., Roble, R.G., Liu, H.-L., Schmidt, H., 2008. Climatology of mesopause region temperature, zonal wind, and meridional wind over Fort Collins, Colorado (41°N, 105°W), and comparison with model simulations. *J. Geophys. Res.* 113, D03105. doi:10.1029/2007JD008697.